BIOCHEMICAL PHARMACOLOGY 73 (2007) 1463–1473

available at www.sciencedirect.com

ScienceDirect

journal homepage: www.elsevier.com/locate/biochempharm

Amino terminal domains of human UDP-glucuronosyltransferases (UGT) 2B7 and 2B15 associated with substrate selectivity and autoactivation

Benjamin C. Lewis [a], *Peter I. Mackenzie* [a], *David J. Elliot* [a], *Brian Burchell* [b], *C. Ramana Bhasker* [a], *John O. Miners* [a,*]

[a] *Department of Clinical Pharmacology, Flinders University and Flinders Medical Centre, Adelaide, Australia*
[b] *Department of Biochemical Medicine, University of Dundee, Dundee, United Kingdom*

ARTICLE INFO

Article history:
Received 2 November 2006
Accepted 18 December 2006

Keywords:
UDP-glucuronosyltransferase
Glucuronidation
Structure–function
Autoactivation
UGT2B7
UGT2B15

ABSTRACT

Despite the important role of UDP-glucuronosyltransferases (UGT) in the metabolism of drugs, environmental chemicals and endogenous compounds, the structural features of these enzymes responsible for substrate binding and selectivity remain poorly understood. Since UGT2B7 and UGT2B15 exhibit distinct, but overlapping, substrate selectivities, UGT2B7–UGT2B15 chimeras were constructed here to identify substrate binding domains. A UGT2B7-15-7 chimera that incorporated amino acids 61–194 of UGT2B15 glucuronidated the UGT2B15 substrates testosterone and phenolphthalein, but not the UGT2B7 substrates zidovudine and 11α-hydroxyprogesterone. Derived apparent K_m values for testosterone and phenolphthalein glucuronidation by UGT2B7-$15_{(61–194)}$-7 were similar in magnitude to those determined for UGT2B15. Moreover, glucuronidation of the non-selective substrate 4-methylumbelliferone (4MU) by UGT2B7-$15_{(61–194)}$-7 and UGT2B15 followed Michaelis–Menten and weak substrate inhibition kinetics, respectively, whereas 4MU glucuronidation by UGT2B7 exhibited sigmoidal kinetics characteristic of autoactivation. Six UGT2B7-15-7 chimeras that incorporated smaller domains of UGT2B15 were subsequently generated. Of these, UGT2B7-$15_{(61–157)}$-7, UGT2B7-$15_{(91–157)}$-7 and UGT2B7-$15_{(61–91)}$-7 glucuronidated 4MU, but activity towards the other substrates investigated here was not detected. Like UGT2B7, the UGT2B7-$15_{(61–157)}$-7, UGT2B7-$15_{(91–157)}$-7 and UGT2B7-$15_{(61–91)}$-7 chimeras exhibited sigmoidal 4MU glucuronidation kinetics. The sigmoidal 4MU kinetic data were well modelled using both the Hill equation and the expression for a two-site model that assumes the simultaneous binding of two substrate molecules at equivalent sites. It may be concluded that residues 61–194 of UGT2B15 are responsible for substrate binding and for conferring the unique substrate selectivity of UGT2B15, while residues 158–194 of UGT2B7 appear to facilitate the binding of multiple 4MU molecules within the active site.

* *Corresponding author at*: Department of Clinical Pharmacology, Flinders Medical Centre, Bedford Park, SA 5042, Australia. Tel.: +61 8 82044131; fax: +61 8 82045114.
E-mail address: john.miners@flinders.edu.au (J.O. Miners).
0006-2952/$ – see front matter
doi:10.1016/j.bcp.2006.12.021

1. Introduction

Glucuronidation, which involves the covalent linkage (or 'conjugation') of glucuronic acid, derived from the cofactor UDP-glucuronic acid (UDPGA), is an essential detoxification and elimination mechanism for a large number of structurally diverse compounds that include drugs, environmental chemicals, endogenous compounds, and the products of phase I metabolism [1–3]. The glucuronidation reaction is catalyzed by UDP-glucuronosyltransferase (UGT), which is known to exist as an enzyme 'superfamily' [4]. Thirty-three human *UGT* genes have been published to date, of which 17 express an active protein [4,5]. Most UGTs have been classified in two subfamilies, UGT1A and UGT2B, based on sequence identity of the encoded proteins. The individual UGTs exhibit distinct, but overlapping, substrate selectivities. However, in the absence of X-ray crystallographic data the structural features of UGTs that confer selectivity remain poorly understood [2,5,6].

The 1A subfamily enzymes are derived from a single gene locus that comprises 13 'first' exons and their associated promoters and 4 common exons [4,7]. Splicing of the independent first exons to the common exons yields transcripts encoding enzymes that have a unique amino terminal domain of 286 residues but an identical carboxyl terminus comprising 245 amino acids, indicating that substrate selectivity of the UGT1A subfamily enzymes is determined by the amino terminus. In contrast, UGT2B subfamily enzymes are encoded by unique genes and therefore differ in sequence throughout the polypeptide chain. However, sequence similarity is greater in the carboxyl terminal half of UGT2B proteins and studies with chimeric proteins suggest that, at least for some enzymes, substrate selectivity is associated with the amino terminus. Exchanging the carboxyl terminal 232 residues of the rat proteins UGT2B2 and UGT2B3 did not the affect substrate selectivity of either enzyme [8], while substituting the carboxyl terminal 231 amino acids of the rabbit enzymes UGT2B16 and UGT2B13 did not alter UGT2B16 substrate selectivity [9]. Similarly, exchanging the carboxyl terminal 230 residues of the human proteins UGT2B4 and UGT2B7 appeared not to alter selectivity, although the activities of the chimeras were lower than the respective parent enzymes [10]. Consistent with these observations, amino acids 96–101 have been implicated in the binding of opioids to UGT2B7 based on NMR analysis and molecular modelling [11,12]. Site-directed mutagenesis data further implicate some residues within the amino terminal domains of UGTs in substrate selectivity, particularly Ser121 of UGT2B17 [13].

Within the UGT2B subfamily, UGT2B7 and UGT2B15 are the enzymes of greatest significance in drug and chemical metabolism. In particular, UGT2B7 glucuronidates numerous opioids and non-steroidal anti-inflammatory drugs, along with epirubicin, valproic acid and zidovudine (AZT) [14–16]. UGT2B15 metabolizes a more limited range of drugs, notably the *S*-enantiomers of the benzodiazepines oxazepam and lorazepam, but has the capacity to glucuronidate plant-derived phenols, anthroquinones and flavonoids [17–19]. Moreover, both glucuronidate hydroxysteroids, and UGT2B7 metabolizes some fatty acids [2,14,17,20]. Of further interest are the sigmoidal glucuronidation kinetics observed for some substrates of UGT2B7. Several compounds, including 4-methylumbelliferone (4MU), exhibit sigmoidal glucuronidation kinetics characteristic of autoactivation (or positive homotropic cooperativity) with UGT2B7 as the enzyme source [18,21,22]. Kinetic data for 4MU glucuronidation by UGT2B7 may be modelled empirically using the Hill equation, and by a two-site model with positive homotropic cooperativity arising from increased binding affinity upon binding of a second substrate molecule [21]. In contrast, 4MU glucuronidation by UGT2B15 does not exhibit autoactivation [21].

The present study sought to investigate the amino terminal domains which confer UGT2B7 and UGT2B15 substrate selectivity and to identify regions of UGT2B7 that contribute to the autoactivation observed with 4MU. Ten UGT2B7/15 chimeras were generated and their ability to glucuronidate 4MU and UGT2B7 and UGT2B15 selective substrates were compared. Residues 61–194 were shown to be involved in UGT2B15 substrate selectivity while amino acids 157–193 of UGT2B7 contributed to the positive homotropic cooperativity observed with 4MU glucuronidation by UGT2B7.

2. Materials and methods

2.1. Chemicals and reagents

11α-Hydroxyprogesterone (11α-OHPro), 4-methylumbelliferone (4MU), 4-methylumbelliferone β-D-glucuronide (4MUG), phenolphthalein (PPN), phenolphthalein β-D-glucuronide (PPNG), testosterone (TST), testosterone β-D-glucuronide (TSTG), zidovudine (AZT), zidovudine β-D-glucuronide (GAZT), and UDP-glucuronic acid trisodium salt (UDPGA) were purchased from Sigma–Aldrich (Sydney, Australia). *Pfu* Turbo Polymerase was from Stratagene (La Jolla, CA, USA) and Shrimp Alkaline Phosphatase was from Roche Diagnostics GmbH (Penzbeg, Germany). Restriction enzymes were supplied by New England Biolabs (Beverly, USA). Dulbecco's modified Eagle's medium (DMEM), MEM non-essential amino acids solution (10 mM; 100×), and penicillin/streptomycin solution (penicillin-G 5000 U/mL–streptomycin sulfate 5000 mg/mL) were purchased from Invitrogen (Carlsbad, USA). Other reagents and solvents were of analytical reagent grade.

2.2. Generation of chimeric UGT constructs

The human UGT2B7 and UGT2B15 cDNAs were isolated as reported previously by Jin et al. [14] and by Monaghan et al. [23], respectively. Throughout this paper the designation of nucleotide and amino acid positions for both UGT2B7 and UGT2B15 are referenced relative to the 5′-ATG start codon. The apparent discrepancy in the numbering of the UGT2B7 and UGT2B15 chimeras is due to the additional glycine positioned at residue 100 of the UGT2B15 protein (Fig. 1). UGT2B7 and UGT2B15 coding sequences were independently cloned into the pBSII SK(+) (Stratagene) vector at *Xho*I and *Xba*I restriction sites. The parent templates were used to generate UGT2B7/2B15 chimeric DNA which was subsequently cloned into the mammalian expression vector pEF-IRES-puro6 for transfection and expression (see Section 2.3). Mutagenesis, to produce

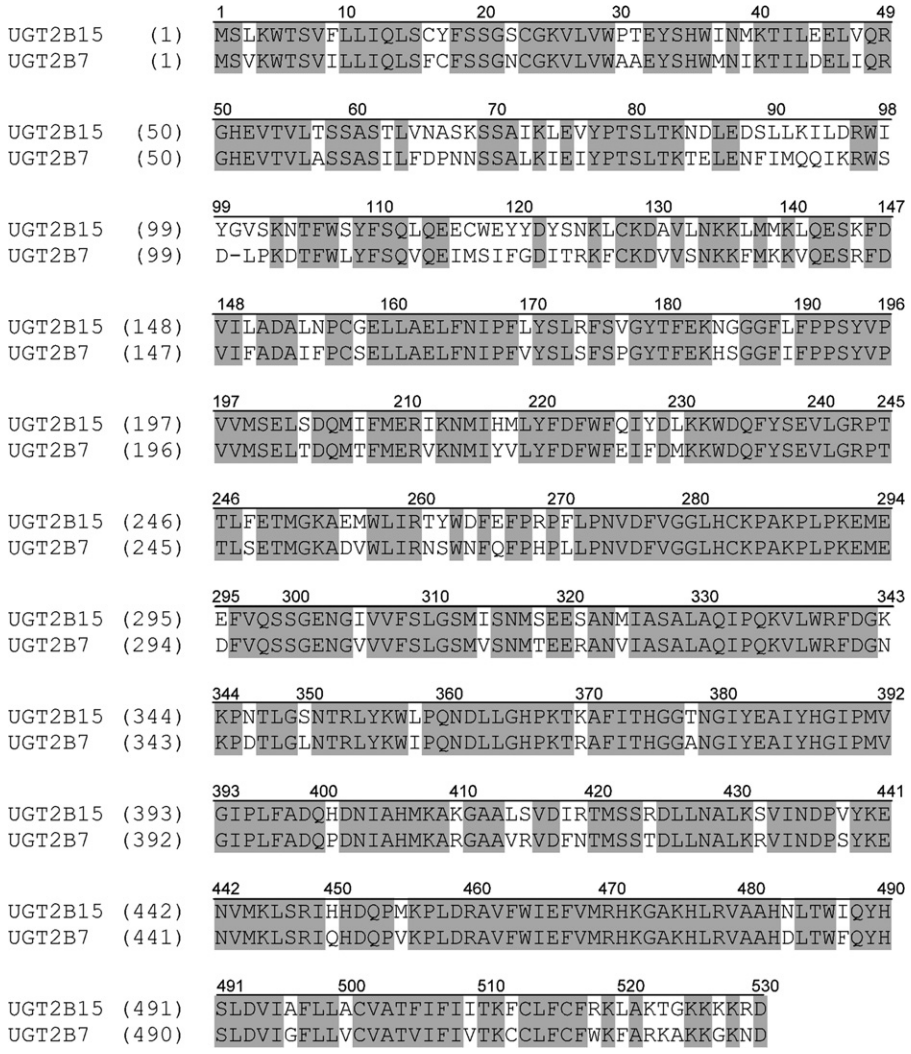

Fig. 1 – Amino acid alignment of UGT2B7 and UGT2B15. Identical residues are shaded. The UGT2B7 and UGT2B15 proteins share 77.7% sequence identity and 86.0% similarity.

the restriction sites necessary for chimera construction (see below), was performed using the QuikChange II Site-directed Mutagenesis protocol (Stratagene) with the primers shown in Table 1. The constructs generated and the positions of restriction sites are shown in Fig. 2. Sequences of all chimeric cDNAs were confirmed by sequence analysis.

2.2.1. *UGT2B7-15 and UGT2B15-7*

The *Xho*I–*Sac*I DNA fragments of the UGT2B7 and UGT2B15 parent templates were exchanged to generate plasmids encoding the amino terminal 298 residues of UGT2B7 and carboxy-terminal 232 residues of UGT2B15, and the reverse chimera containing the amino terminal 299 residues of UGT2B15 and carboxy-terminal 232 residues of UGT2B7.

2.2.2. *UGT2B7-15$_{(61–194)}$-7 and UGT2B15-7$_{(61–193)}$-15*

Silent (i.e. not resulting in a change to the amino acid sequence) *Nhe*I restriction sites at nucleotide 180 were engineered into the UGT2B7 and UGT2B15 parent templates (Table 1). In addition, a silent *Sna*BI restriction site corresponding to that already present in UGT2B7 was engineered into the UGT2B15 cDNA at nucleotide 585 (Table 1). The respective *Nhe*I–*Sna*BI fragments, which incorporated 396 and 399 nucleotides of the parent UGT2B7 and UGT2B15 templates, respectively, were exchanged to generate the UGT2B7-15$_{(61–194)}$-7 and UGT2B15-7$_{(61–193)}$-15 chimeras.

2.2.3. *UGT2B7-15$_{(91–194)}$-7*

*Nde*I restriction sites at nucleotide 272 were engineered into the UGT2B7 parent template and the UGT2B7-15$_{(61–194)}$-7 chimera (Table 1). The *Xho*I–*Nde*I fragment of UGT2B7-15$_{(61–194)}$-7 was exchanged for that of the UGT2B7 parent. Subsequent mutagenesis eliminated the *Nde*I restriction site to restore the desired sequence at the UGT2B7–UGT2B15 junction (Table 1).

2.2.4. *UGT2B7-15$_{(61–157)}$-7*

Silent *Pst*I restriction sites at nucleotides 469 and 472 were, respectively, incorporated into the UGT2B7 and UGT2B15 parent templates containing the engineered *Nhe*I site at nucleotide 180 (Table 1). The *Nhe*I–*Pst*I 288 nucleotide fragment of the UGT2B7 parent template (nucleotides 183–469) was exchanged with that of the UGT2B15 parent template (nucleotides 183–472).

Table 1 – Oligonucleotides used for the construction of UGT2B7–UGT2B15 chimeras

UGT chimera	Template	Oligonucleotide (5′–3′ of the leading strand)	Restriction site engineered
2B7-15$_{(61–194)}$-7	2B7	GGTGACTGTACTGGCATCTTCAGCT**AG**CATTCTTTTTGATCCC	*Nhe*I
2B15-7$_{(61-193)}$-15	2B15	GGTGACTGTGTTGACATCTTCGGCT**AG**CACTCTTGTCAATGCC	*Nhe*I
	2B15	GGATTTCTGTTCCCTCCTTCCTA**CG**TACCTGTTGTTATGTCAG	*Sna*BI
2B7-15$_{(91–194)}$-7	2B7	CTGAGTTGGAGAATTTCATC**CATATG**CAGATTAAGAGATGG	*Nde*I
	2B7-15$_{(61–194)}$-7	CTAAAAATGATTTGGAAGATTCTCTT**CATATG**ATTCTCGATAGATGGATATAT	*Nde*I
	2B7-15$_{(91–194)}$-7 *Nde*I	GGAGAATTTCATC**ATGAAA**ATTCTCGATAGATGGATATATGG	*
2B7-15$_{(61–157)}$-7	2B7 *Nhe*I	GCAGATGCTATTTTTCCCTG**C**AGTGAGCTGCTGGCTGAGC	*Pst*I
	2B15 *Nhe*I	GCAGATGCCCTTAATCCCTG**CA**GTGAGCTACTGGCTG	*Pst*I
2B7-15$_{(157–193)}$-7	2B7	TTTTTGCAGATGCTATTTTTCCCT**CTCGA**GAGCTGCTGGCTGAGC	*Xho*I
	2B7-15$_{(61–194)}$-7	CATTCTGGCAGATGCGCCTTAATCCT**CTCGA**GGTGAGCTACTGGCTG	*Xho*I
	2B7-15$_{(157–193)}$-7 *Xho*I	GCAGATGCTATTTTTCCCT**GTTAGT**GAGCTACTGGCTGAACTATTTAACATACC	*
2B7-15$_{(61–91)}$-7	2B7-15$_{(61–91)}$-7 *Nde*I	GATTTGGAAGATTCTCTTT**CTACA**GCAGATTAAGAGATGGTCAGACC	*
2B7-15$_{(61-91)}$-7-15$_{(157-193)}$-7	2B7-15$_{(61–91)}$-7	TTTTTGCAGATGCTATTTTTCCCT**CTCGA**GAGCTGCTGGCTGAGC	*Xho*I
	2B7-15$_{(61–91)}$-7–15$_{(157–193)}$-7 *Xho*I	GCAGATGCTATTTTTCCCT**GTTAGT**GAGCTACTGGCTG	*
	2B7-15$_{(61–91)}$-7–15$_{(157–193)}$-7 *Nde*I	GATTTGGAAGATTCTCTTT**CTACA**GCAGATTAAGAGATGGTCAGACC	*

Nucleotides used to introduce restriction sites are bolded. Asterisks show oligonucleotides used to restore the native UGT2B7–UGT2B15 junction.

2.2.5. *UGT2B7-15$_{(91–157)}$-7*

The UGT2B7 parent template containing the *Nde*I restriction site (see UGT2B7-15$_{(91–194)}$-7) and an engineered *Nde*I site in UGT2B7-15$_{(61–157)}$-7 at nucleotide 272 were utilized in conjunction with *Xho*I to replace the amino terminal 272 nucleotides of UGT2B7-15$_{(61–157)}$-7 with those of UGT2B7. Subsequent mutagenesis eliminated the *Nde*I restriction site to restore the desired sequence at the UGT2B7–UGT2B15 junction (see UGT2B7-15$_{(91–194)}$-7).

2.2.6. *UGT2B7-15$_{(157–193)}$-7*

An internal *Xho*I restriction site was engineered into the UGT2B7 parent template and the UGT2B7-15$_{(61–194)}$-7 chimera at nucleotide 467 (Table 1) in order to exchange the first 156 residues of UGT2B7-15$_{(61–194)}$-7 with the corresponding sequence of UGT2B7. Subsequent mutagenesis eliminated the *Xho*I restriction site to restore the desired sequence at the UGT2B7–UGT2B15 junction (Table 1).

2.2.7. *UGT2B7-15$_{(61–91)}$-7*

The UGT2B7 parent template containing the *Nde*I restriction site and the UGT2B7-15$_{(61–194)}$-7 chimera with an engineered *Nde*I restriction site at nucleotide 272 (see UGT2B7-15$_{(91–194)}$-7) were utilized to replace the carboxy-terminal 440 residues of UGT2B7-15$_{(61–194)}$-7 with the carboxy-terminal 439 residues of UGT2B7. Subsequent mutagenesis eliminated the *Nde*I restriction sites to restore the desired residues (Table 1).

2.2.8. *UGT2B7-15$_{(61–91)}$-7–15$_{(157–193)}$-7*

*Xho*I restriction sites engineered into UGT2B7-15$_{(61–91)}$-7 and UGT2B7-15$_{(157–193)}$-7 constructs at nucleotide 467 were utilized to exchange the amino terminal 156 residues of UGT2B7-15$_{(157–193)}$-7 with those of UGT2B7-15$_{(61–91)}$-7. The introduced *Xho*I restriction sites were eliminated by mutagenesis, as previously described (Table 1).

2.3. *Expression of recombinant UGT proteins*

The individual parent and chimeric UGT2B cDNAs were stably expressed in HEK293 cells as described by Sorich et al. [24] and Uchaipichat et al. [21]. Cells were transfected with cDNAs cloned in the pEF-IRES-puro6 expression vector [25], and incubated in a humidified incubator with an atmosphere of 5% CO_2 at 37 °C in DMEM prepared in the presence of sodium bicarbonate (44 mM), MEM non-essential amino acids (0.1 mM) and penicillin/streptomycin (100 U/mL). Media were additionally supplemented with puromycin (1.0 mg/L) for selection and fetal bovine serum (10%). Cells were grown to no more than 90% confluency. The conditioned medium was decanted and the cultured cells washed (3×) with pre-chilled (4 °C) phosphate buffered saline (pH 7.4). Cell pellets were resuspended in a storage buffer (10 mM K_2HPO_4/KH_2PO_4, pH 7.4, 0.1 mM EDTA, 0.5 mM DTT) and kept at −80 °C until use. Cells expressing the UGT2B7 and UGT2B15 chimeric proteins were lysed by sonication [21].

2.4. *Immunoblotting*

Equal amounts of HEK293 cell lysate protein (50 μg) were subjected to 10% SDS-PAGE, transferred onto nitrocellulose,

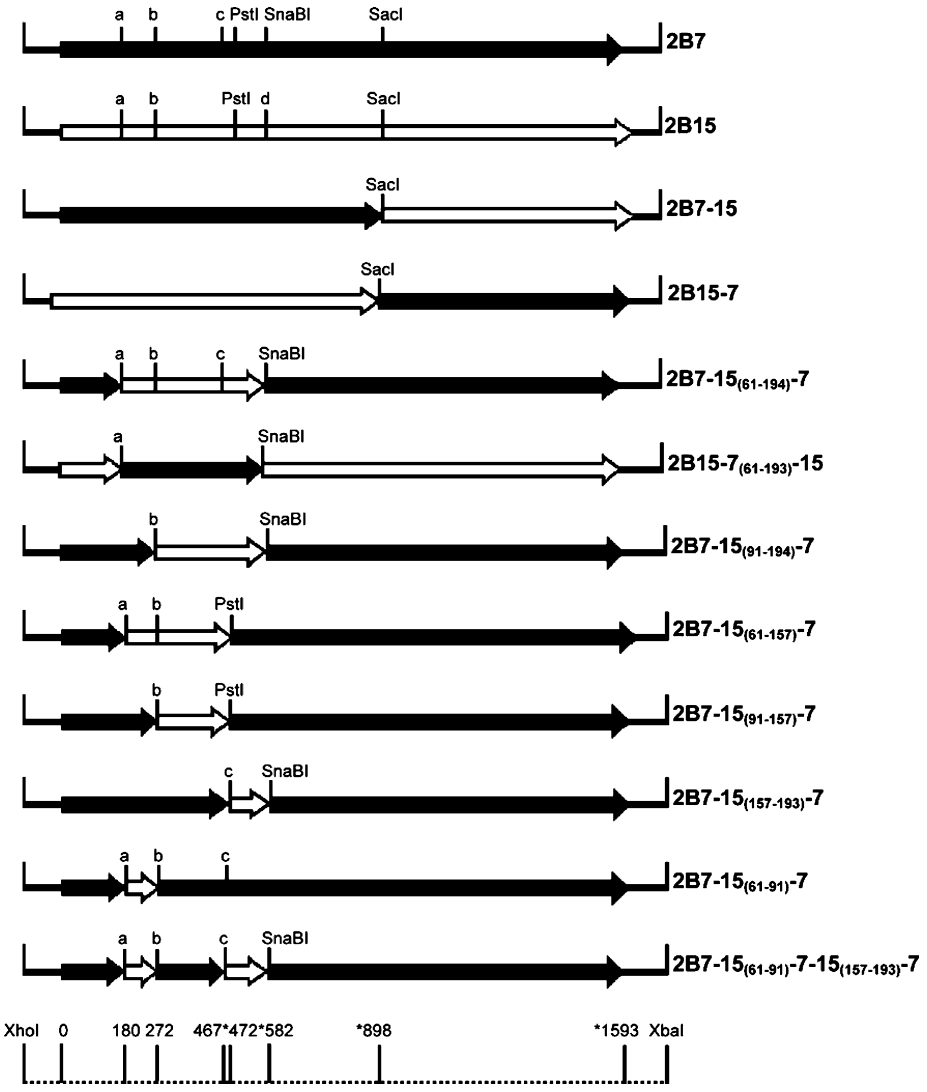

Fig. 2 – UGT2B7–UGT2B15 chimeras. Arrow heads show the junctions between various UGT 2B7 and 2B15 coding sequences. The 5′ and 3′ flanks give the positions of *Xho*I and *Xba*I restriction sites, respectively, which were used for the directional transfer of cDNAs into the mammalian expression vector pEF-IRES-puro6. Positions marked a, b, c and d show the positions of the engineered *Nhe*I, *Nde*I, *Xho*I, and *Sna*BI restriction sites, respectively, that were employed to construct chimeric cDNAs. Engineered sites were restored to the native sequence by site-directed mutagenesis (Table 1). *Pst*I and *Sac*I sites were native to the UGT 2B7 and 2B15 sequences, while the *Sna*BI site occurred only in UGT2B7. Asterisks give the nucleotide length of those constructs containing the additional amino acid (at position 100) of UGT2B15. Chimeras without this additional residue have 469, 895, or 1590 nucleotides in the respective asterisked sites.

and probed with anti-goat UGT2B primary antiserum (1:2000 dilution) [26] and rabbit anti-goat IgG (1:2000 dilution; H +L - HRP) as the secondary antibody (Southern Biotechnology Associates Inc., Birmingham USA). Membrane-bound peptides conjugated with HRP were detected by chemiluminescence (Roche Diagnostics, Mannheim, Germany) and subsequently exposed to Omat autoradiographic film (Kodak). Band intensities were measured using a GS-700 imaging densitometer (Biorad, CA, USA).

2.5. *Enzyme assays*

4MU is a non-selective UGT substrate [21]. In contrast, AZT and 11α-OHPro are glucuronidated by UGT2B7 and not UGT2B15, and the reverse selectivity occurs with TST and PPN (see Section 3). Screening for 4MU, TST, PPN, AZT and 11α-OHPro glucuronidation by UGT2B7, UGT2B15 and the chimeric proteins was performed at 37 °C in a total incubation volume of 200 μL. Incubation mixtures contained HEK293 cell lysate protein, test substrate, 0.1 M phosphate buffer (0.1 M, pH 7.4), $MgCl_2$ (4 mM) and UDPGA (5 mM; >10-times the UDPGA K_m for both enzymes). Incubation conditions varied for each test substrate. *4MU*: protein 1.0 mg/mL, incubation time 90 min, 4MU concentrations 50, 300 and 1000 μM. *TST*: protein 0.5 mg/mL, incubation time 90 min, TST concentrations 2.5, 10 and 50 μM. *PPN*: protein 0.5 mg/mL, incubation time 20 min, PPN concentrations 2.5, 10 and 50 μM. *AZT*: protein 1.0 mg/mL, incubation time 120 min, AZT concentrations 100, 500 and

3000 μM. *11α-OHPro*: protein 0.5 mg/mL, incubation time 20 min, 11α-OHPro concentrations 2.5, 10 and 50 μM. 4MU and AZT were dissolved in water. TST, PPN and 11α-OHPro stock solutions were prepared in methanol such that the final concentration of solvent in incubation mixtures was 1%. All reactions were initiated, following a 5 min pre-incubation at 37 °C in a shaking water bath, by the addition of UDPGA. The reactions were terminated by the addition of 2 μL of perchloric acid (11.6 M) and cooling on ice. The samples were then vortex mixed, centrifuged (3000 × *g*, 10 °C) and an aliquot of the supernatant fraction was analyzed by HPLC.

For the determination of kinetic parameters, product formation was optimized for linearity with respect to cell lysate protein concentration and incubation time with UGT2B7 and UGT2B15 as the enzyme sources. Experiments were performed as described above with the following protein concentrations, incubation times and substrate concentrations. *AZT glucuronidation by UGT2B7*: protein 1.5 mg/mL, incubation time 60 min, and AZT concentration range 100–3000 μM. *11α-OHPro glucuronidation by UGT2B7*: protein 0.5 mg/mL, incubation time 20 min, and 11α-OHPro concentration range 1–50 μM. *4MU glucuronidation by UGT2B7*, *UGT2B7-15*$_{(61–193)}$*-7*, *UGT2B7-15*$_{(61–156)}$*-7 and UGT2B7-15*$_{(91–157)}$*-7*: protein 0.2 mg/mL, incubation time 90 min, and 4MU concentration range 25–1500 μM. *4MU glucuronidation by UGT2B7-15*$_{(61–90)}$*-7*: protein 0.6 mg/mL, incubation time 90 min, and 4MU concentration range 25–2400 μM. *4MU glucuronidation by UGT2B15*: protein 0.5 mg/mL, incubation time 90 min, and 4MU concentration range 25–1500 μM. *TST glucuronidation UGT2B15 and UGT2B7-15*$_{(61–193)}$*-7*: protein 0.2 mg/mL, incubation time 90 min, and TST concentration range 1–40 μM. *PPN glucuronidation by UGT2B15 and UGT2B7-15*$_{(61–193)}$*-7*: protein 0.2 mg/mL, incubation time 20 min, and PPN concentration range 0.5–25 μM. Duplicate determinations were performed for least eight substrate concentrations within the ranges specified above.

2.6. HPLC conditions

The glucuronides of each test substrate were separated and quantified by reversed phase HPLC using an Agilent 1100 series HPLC system (Aglient Technologies, Sydney, Australia) which consisted of a quaternary gradient pump, autosampler and UV detector. The HPLC system was fitted with a NovaPak C18 column (150 mm × 3.9 mm, Waters, Milford, MA, USA). Chromatography conditions are given in Table 2. The identity of glucuronides was confirmed by comparison with an authentic standard where available (4MUG, AZTG, TSTG, PPNG) and by β-glucuronidase hydrolysis of incubation mixtures (all substrates).

2.7. Data analysis

Data points represent the mean of duplicate estimates. Kinetic constants for 4MU, AZT, 11α-OHPro, TST and PPN glucuronidation by UGT2B7, 2B15, and each chimera were obtained by fitting untransformed experimental data to kinetic models using the non-linear curve fitting program EnzFitter (Biosoft, Cambridge, UK). Parameter standard error estimates, 95% confidence intervals, *F*-statistic and r^2 values were used to determine the goodness-of-fit of the kinetic models. Models used included:

- The Michaelis–Menten equation:

$$v = \frac{V_{max}[S]}{K_m[S]} \quad (1)$$

Table 2 – Chromatography conditions for the HPLC analysis of glucuronides

Substrate	Detector wavelength (nm)	Mobile phase gradient[a]		Retention times (min)		Calibration standard	Calibration range (μM)
		Time (min)	Composition				
4MU	316	0–3 3–4 4–10	96% A, 4% E 70% A, 30% E 96% A, 4% E	4MUG 4MU	3.5 5.8	4MUG	0.5–40
TST	241	0–1 1–9 9–9.2 9.2–15	96% B, 4% E 35% B, 65% E 35% B, 65% E 96% B, 4% E	TSTG TST	5.2 9.5	TST[b]	1–5
PPN	230	0–3.4 3.4–4.4 4.4–10	84% A, 16% E 55% A, 45% E 84% A, 16% E	PPNG PPN	3.5 5.9	PPNG	0.5–10
AZT	267	0–10	100% C	AZTG AZT	3.1 6.3	AZTG	1–10
11α-OHP	241	0–1 1–7 7–10	85% D, 15% E 50% D, 50% E 85% D, 15% E	11α-OHPG 11α-OHP	4.2 7.7	11α-OHP[b]	1–5

[a] Mobile phase composition: (A) aqueous triethylamine (10 mM, adjusted to pH 2.5 with 12 M perchloric acid) containing 10% acetonitrile; (B) water containing 5% acetonitrile; (C) aqueous acetic acid (20 mM) containing 10% acetonitrile; (D) 20 mM sodium acetate buffer (pH 4.3) containing 5% acetonitrile; (E) acetonitrile.

[b] The use of TST as the calibration standard for TSTG formation was validated by confirming that TST and TSTG have similar molar extinction coefficients at 241 nm. An authentic standard of 11α-OHPG was not available, but it is expected that 11α-OHP and 11α-OHPG would have similar molar extinction coefficients at 241 nm based on data for other steroidal substrates.

where v is the rate of reaction, V_{max} the maximum velocity, K_m the Michaelis constant (substrate concentration at 0.5 V_{max}), and [S] is the substrate concentration.

- Substrate inhibition model:

$$v = \frac{V_{max}}{1 + (K_m/[S]) + [S]/K_{si}} \quad (2)$$

where K_{si} is the constant describing the substrate inhibition interaction.

- The Hill equation, which describes sigmoidal kinetics:

$$v = \frac{V_{max}[S]^n}{S_{50}^n + [S]^n} \quad (3)$$

where S_{50} is the substrate concentration resulting in 50% of V_{max} (analogous to K_m in previous equations) and n is the Hill coefficient.

Sigmoidal kinetic data were additionally fitted to the two-site model described by Houston and Kenworthy [27]. The model is based on a steady-state rapid equilibrium approach and assumes two identical binding sites:

$$\frac{v}{V_{max}} = \frac{[S]/K_s + \beta[S]^2/\alpha K_s^2}{1 + 2[S]/K_s + [S]^2/\alpha K_s^2} \quad (4)$$

where K_s is binding affinity and α and β are interaction factors which reflect changes in K_s and product formation (K_p), respectively. For positive homotropic cooperativity (sigmoidal kinetics), V_{max} is equivalent to $2K_p[E]_t$, where $[E]_t$ is the total enzyme concentration, and hence $\beta = 2$ for this type of kinetics.

3. Results

3.1. Substrates

4MU is a substrate of both UGT2B7 and UGT2B15 [21], and is useful for screening the activity of chimeras. However, it was necessary to identify compounds that differentiated the substrate selectivity of each hybrid protein. Based on literature data, AZT, 11α-OHPro, TST, and PPN were evaluated for glucuronidation by UGT2B7 and UGT2B15. Consistent with previous reports [18,28] only UGT2B7 glucuronidated AZT; rates of GAZT formation were 6.8, 23 and 36 pmol/min mg at substrate concentrations of 100, 500 and 3000 μM, respectively. UGT2B7 shows activity towards 11α-OHPro [29]. UGT2B15 was shown here not to metabolize 11α-OHPro, while rates of glucuronidation of this compound by UGT2B7 were 61, 171 and 260 pmol/min mg at 2.5, 10 and 50 μM, respectively. Conversely, PPN is known to be a substrate of UGT2B15 [17] but there are no reports of metabolism by UGT2B7. Here, UGT2B15, but not UGT2B7, glucuronidated PPN; rates of PPN glucuronidation were 15, 23 and 26 pmol/min mg at substrate concentrations of 2.5, 10 and 50 μM, respectively. The 'relative' V_{max} values for TST glucuronidation by UGT2B7 and UGT2B15 have previously been reported as 0.4 and 4.4 pmol/min mg, respectively [20]. Rates of TST glucuronidation by UGT2B15 measured here were 2.0, 5.5 and 8.2 pmol/min mg at substrate concentrations of 2.5, 10 and 50 μM, respectively. Although a peak corresponding to TST glucuronide was observed in chromatograms from incubations of TST (10 and 50 μM) and UGT2B7, concentrations were below the limit of quantification (equivalent to 0.5 pmol/min mg) of the HPLC assay employed. Kinetic parameters for 4MU, AZT and 11α-OHPro glucuronidation by UGT2B7 and 4MU, PPN and TST glucuronidation were subsequently determined over a concentration range that spanned the apparent K_m (or S_{50}) for each substrate.

3.2. Expression and activities of UGT2B7–UGT2B15 chimeras

All of the chimeras shown in Fig. 2 expressed in HEK293 cells. Levels of expression of UGT2B15, UGT2B7-15, UGT2B15-7, UGT2B7-15$_{(61–194)}$-7, UGT2B15-7$_{(61–193)}$-15, UGT2B7-15$_{(61–157)}$-7, UGT2B7-15$_{(91–157)}$-7, UGT2B7-15$_{(61–91)}$-7, UGT2B7-15$_{(91–194)}$, UGT2B7-15$_{(157–193)}$-7, and UGT2B7-15$_{(61–91)}$-7–15$_{(157–193)}$-7 relative to UGT2B7, were 0.86, 0.43, 0.54, 0.65, 0.18, 0.29, 0.38, 0.59, 0.28, 0.33, and 0.12, respectively (Fig. 3). The antibody employed recognises all UGT2B subfamily proteins. V_{max} values reported in Tables 3 and 4 have been normalized for expression relative to UGT2B7, although we have refrained from making quantitative comparisons involving this parameter given the inability to validate equivalent recognition of all proteins by the antibody.

The UGT2B7-15 and UGT2B15-7 chimeras, constructed using a common *Sac*I site at nucleotide 898, were devoid of activity towards 4MU and the other substrates investigated here. Since UGT 2B7 and 2B15 exhibit greatest sequence dissimilarity in the amino terminal half of the proteins (Fig. 1), chimeras were constructed whereby residues 61–193 of UGT2B7 and 61–194 of UGT2B15 were exchanged. 4MU glucuronidation by UGT2B7 exhibits sigmoidal kinetics (Fig. 4A), which may be modelled using the Hill equation

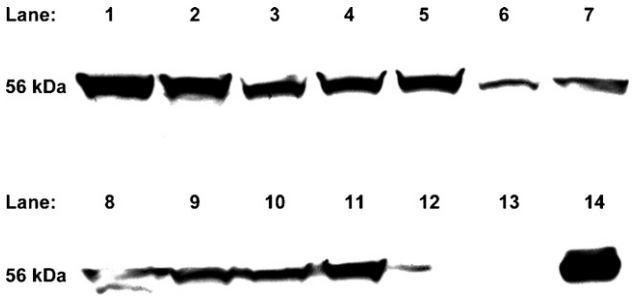

Fig. 3 – Western blot analysis of UGT2B7 and UGT2B15 chimera expression in HEK293 cells. Cell lysate (50 μg) was resolved by SDS-PAGE, blotted on to nitrocellulose, and probed with anti-UGT antiserum. Bands: UGT2B7 (lane 1), UGT2B15 (lane 2), UGT2B7-15 (lane 3), UGT2B15-7 (lane 4), UGT2B7-15$_{(61–194)}$-7 (lane 5), UGT2B15-7$_{(61–193)}$-15 (lane 6), UGT2B7-15$_{(91-194)}$-7 (lane 7), UGT2B7-15$_{(61–157)}$-7 (lane 8), UGT2B7-15$_{(91–157)}$-7 (lane9), UGT2B7-15$_{(157–193)}$-7 (lane 10), UGT2B7-15$_{(61–91)}$-7 (lane 11), UGT2B7-15$_{(61–91)}$-7–15$_{(157–193)}$-7 (lane 12), untransfected HEK293 cell lysate (lane 13), and human liver microsomal protein (7.5 μg) (lane 14).

Table 3 – Kinetic constants (apparent K_m or S_{50} (μM), V_{max} (pmol/min mg) and Hill coefficient (η)) for 4MU, TST, PPN, AZT and 11α-OHPro glucuronidation derived from fitting experimental data to empirical models

Enzyme	4MU[a]			TST[b]		PPN[b]		AZT[b]		11α-OHPro[b]	
	S_{50} (or K_m)	V_{max}[c]	n	K_m	V_{max}[c]	K_m	V_{max}[c]	K_m	V_{max}[c]	K_m	V_{max}[c]
2B7	369 ± 2.2	271 ± 1	1.60 ± .02	na	na	na	na	478 ± 14	43 ± 0.5	7.4 ± 0.3	297 ± 4
2B15	417 ± 0.5	17 ± 0.01		6.5 ± 0.02	9.7 ± 0.01	2.2 ± 0.04	34 ± 0.14	na	na	na	na
2B7-15 $_{(61–194)}$-7	358 ± 12	198 ± 6		3.0 ± 0.19	2.2 ± 0.05	1.6 ± 0.05	45 ± 0.30	na	na	na	na
2B7-15 $_{(61–157)}$-7	360 ± 13	715 ± 10	1.58 ± 0.07	na[d]	na	na	na	na	na	na	na
2B7-15 $_{(91–157)}$-7	356 ± 9	545 ± 7	1.62 ± 0.05	na	na	na	na	na	na	na	na
2B7-15$_{(61–91)}$-7	872 ± 40	54 ± 1.6	1.66 ± 0.07	na	na	na	na	na	na	na	na

Values are shown as the parameter estimate ± S.E. of the parameter fit.
[a] Initial rate data for 4MU glucuronidation were best fitted to the Hill equation except for: UGT2B15, which was fitted to the substrate inhibition equation (K_{si} 1402 ± 2.4 μM); and UGT2B7-15$_{(61–194)}$-7, which was fitted to the Michaelis–Menten equation.
[b] Data fitted to the Michaelis–Menten equation.
[c] V_{max} values corrected for expression relative to UGT2B7.
[d] na = no activity (i.e. undetectable glucuronide formation by the enzyme/chimera).

Table 4 – Kinetic constants (K_s (μM), V_{max} (pmol/min mg) and α) for 4MU glucuronidation derived from fitting experimental data to a two-site model

Enzyme	K_s	V_{max}	α
2B7	1798 ± 28	302 ± 2	0.06 ± 0.002
2B7-15$_{(61–157)}$-7	1608 ± 45	716 ± 2	0.05 ± 0.003
2B7-15$_{(91–157)}$-7	1866 ± 192	547 ± 6	0.04 ± 0.008
2B7-15$_{(61–91)}$-7	4740 ± 805	53 ± 1	0.04 ± 0.013

Values are shown as the parameter estimate ± S.E. of the parameter fit.

(Eq. (3), Section 2.7); the derived S_{50} was 369 μM (Table 3). In contrast, 4MU glucuronidation by UGT2B15 followed 'weak' substrate inhibition kinetics (Fig. 4B), with derived apparent K_m and K_{si} values of 417 and 1402 μM, respectively. The UGT2B7-15$_{(61–194)}$-7 chimera, but not UGT2B15-7$_{(61–193)}$-15, glucuronidated 4MU. 4MU glucuronidation by UGT2B7-15$_{(61–194)}$-7 exhibited Michaelis–Menten kinetics (apparent K_m 358 μM; Table 3). UGT2B7-15$_{(61–194)}$-7 was further shown to glucuronidate PPN and TST, but not AZT and 11α-OHPro. The glucuronidation of both substrates was well modelled using the Michaelis–Menten equation, as was also observed with UGT2B15 as the enzyme source (Fig. 4E and F). Furthermore, derived apparent K_m values for PPN and TST glucuronidation by UGT2B7-15$_{(61–194)}$-7 were similar in magnitude to those determined for UGT2B15 (Table 3).

UGT2B7-15-7 chimeras that incorporated smaller domains of UGT2B15 were subsequently generated: UGT2B7-15$_{(61–157)}$-7, UGT2B7-15$_{(91–157)}$-7, UGT2B7-15$_{(61–91)}$-7, UGT2B7-15$_{(91–194)}$-7, UGT2B7-15$_{(157–193)}$-7, and UGT2B7-15$_{(61–91)}$-7–15$_{(157–193)}$-7. Of these, only the first three glucuronidated 4MU, but activity towards the other substrates investigated here was not detected. Given the relatively lower expression of UGT2B7-15$_{(91–194)}$-7, UGT2B7-15$_{(157–193)}$-7, UGT2B7-15$_{(61–91)}$-7–15$_{(157–193)}$-7, the content of HEK293 cell lysates expressing these proteins included in incubations was increased to 3 mg/mL but activity was still undetectable. UGT2B7-15$_{(61–157)}$-7, UGT2B7-15$_{(91–157)}$-7 and UGT2B7-15$_{(61–91)}$-7 all exhibited sigmoidal 4MU glucuronidation kinetics that were analyzed initially using the Hill equation (Table 3).

3.3. *Two-site kinetic modelling of 4MU glucuronidation kinetics*

Kinetic data for 4MU glucuronidation by UGT2B7 and UGT2B7-15$_{(61–157)}$-7, UGT2B7-15$_{(91–157)}$-7 and UGT2B7-15$_{(61–91)}$-7 were further modelled using the expression for a two-site model (Eq. (4), Section 2.7). Derived kinetic constants are shown in Table 4. Goodness-of-fit parameters (*F*-statistic, S.E. of fit (as a percentage) and r^2 values) for fitting data to the two-site model were equivalent to, or better than, fitting to the Hill equation (data not shown).

4. Discussion

Chimeragenesis has been used previously to investigate aglycone and cofactor binding domains of rat, rabbit and human UGT2B subfamily enzymes [8–10]. Exchanging the carboxyl terminal 230–232 residues of UGT 2B2 and 2B3, UGT

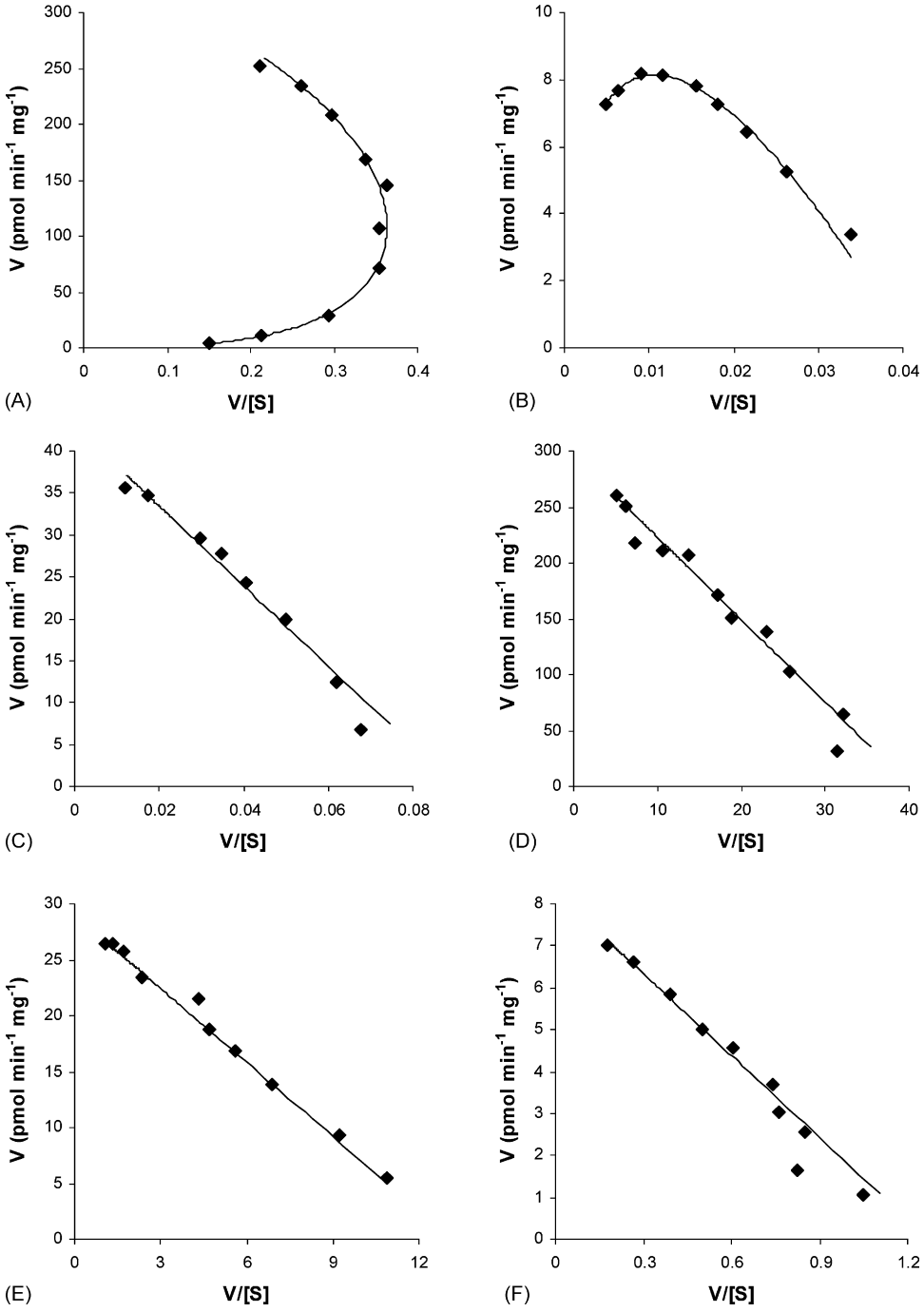

Fig. 4 – Eadie–Hofstee plots for: 4-methylumbelliferone glucuronidation by UGT2B7 (panel A) and UGT2B15 (panel B); zidovudine (panel C) and 11α-hydroxyprogesterone (panel D) by UGT2B7; and phenolphthalein (panel E) and testosterone (panel F) glucuronidation by UGT2B15.

2B13 and 2B16, and UGT 2B4 and 2B7 generally resulted in the synthesis of hybrid proteins that retained aglycone selectivity, consistent with the hypothesis that aglycone selectivity is associated with amino terminal residues. Here, exchanging the amino terminal 298 or 299 residues of UGT2B7 and UGT2B15 resulted in proteins that were devoid of enzyme activity.

UGT2B7 and UGT2B15 share 78% amino acid identity (Fig. 1). However, identity is greatest in the carboxyl terminal domain. For example, identity is 72% between residues 1 and 300 and 84% between residues 301 and 530. Between residues 60 and 194, identity decreases to 59%. Thus, UGT2B7-15$_{(61–194)}$-7 and UGT2B15-7$_{(61–193)}$-15 chimeric proteins were synthesized; of these, only the former was active. Notably, UGT2B7-15$_{(61–194)}$-7 glucuronidated the UGT2B15 substrates PPN and TST, but not the UGT2B7 substrates AZT and 11α-OHPro. Moreover, apparent K_m values for PPN and TST glucuronidation by UGT2B7-15$_{(61–194)}$-7 were similar in magnitude. Other similarities were

observed between these proteins with 4MU as the substrate. 4MU glucuronidation by UGT2B7 and UGT2B15 exhibit sigmoidal and weak substrate inhibition kinetics, respectively. Glucuronidation of this compound by the chimera followed Michaelis–Menten kinetics, with a derived apparent K_m similar to that observed for UGT2B15. Taken together, these observations indicate that residues 60–194 of UGT2B15 are associated with substrate selectivity and binding.

Chimeras incorporating smaller regions of UGT2B15 (residues 61–157, 91–157, 61–91, 91–194, 157–193, and 61–91 plus 157–193) were generated to further explore potential binding domains. While none of these glucuronidated PPN and TST, the chimeras that included residues 158–193 of UGT2B7 (viz. 61–157, 91–157, 61–91) glucuronidated 4MU. Like UGT2B7, the 61–157, 91–157 and 61–91 chimeras exhibited sigmoidal 4MU glucuronidation kinetics (cf. weak substrate inhibition for UGT2B15). Kinetic data were initially modelled using the Hill equation. The Hill coefficient (n), which indicates the degree of sigmoidicity, was similar for UGT2B7 and the three chimeras. Derived S_{50} values for 4MU glucuronidation by UGT2B7 and the 61–157 and 91–157 chimeras were also similar (356–369 μM), while the S_{50} for UGT2B7-$15_{(61–91)}$-7 was somewhat higher (872 μM). These data suggest that residues 158–193 of UGT2B7 contribute to the sigmoidal 4MU glucuronidation kinetics. Clearly, however, residues outside this domain are necessary for UGT2B7-like activity towards the prototypic substrates AZT and 11α-OHPro.

We have demonstrated recently [21] that the sigmoidal 4MU glucuronidation kinetics observed with UGT2B7 are equally well modelled by both the Hill equation and a 'mechanistic' model that assumes binding of substrate (aglycone) at two equivalent sites [27]. The autoactivation characteristic of 4MU glucuronidation by UGT2B7 results from increased binding affinity for a second substrate molecule in the two substrate bound complex, such that K_S changes by a factor $\alpha < 1$. Fitting data for 4MU glucuronidation by UGT2B7 and the 61–157, 91–157 and 61–91 chimeras gave essentially identical values of α (0.04–0.06), consistent with marked cooperativity. As observed with fitting to the Hill equation, derived K_S values for 4MU glucuronidation by UGT2B7 and the 61–157 and 91–157 chimeras were similar (1608–1866 μM), while the K_S for UGT2B7-$15_{(61–91)}$-7 was higher (4740 μM). The kinetic analysis of the 61–157, 91–157 and 61–91 chimeras suggests that residues 158–194 of UGT2B7 are critical for facilitating the binding of two 4MU molecules in the active site. Whether this sequence alters the architecture of the active site to accommodate two substrate molecules or acts as a dimerization domain is unclear. There is evidence to suggest that some UGTs may form homo- and hetero-dimers [30–33]. Importantly, deletion of residues 152–180 of UGT1A1 has been shown to abolish homo-dimerization of this enzyme [34]. Extensive non-specific binding of compounds to the microsomal membrane may give rise to sigmoidal kinetics, especially when the microsomal protein content present in incubations varies with substrate [35]. However, non-specific binding is not the cause of differences in kinetic properties observed between enzymes and chimeras with 4MU as the substrate since 4MU binds negligibly to HEK293 cell lysate (A Rowland and JO Miners, unpublished data).

As indicated previously, exchanging the carboxyl terminal 230–232 residues of UGT 2B2 and 2B3, UGT 2B13 and 2B16, and UGT 2B4 and 2B7 generally resulted in the synthesis of hybrid proteins that retained enzyme activity. UGT2B4-7 and UGT2B7-4 chimeras constructed using the same common *Sac*I employed in this work were both reported to glucuronidate 4-hydroxyestrone and hyodeoxycholic acid [10]. However, glucuronidation activity was extremely low necessitating a 16 h incubation; rates of 4-hydroxyestrone and hyodeoxycholic acid by the UGT2B4-7 and UGT2B7-4 chimeras ranged from 0.02 to 0.35 pmol/min mg. Activities were also low when the carboxyl terminal residues from position 385 were exchanged, although there was little effect on activity from exchanging carboxyl terminal residues from position 469. Li et al. [9] exchanged the amino terminal 231 residues of the rabbit enzymes UGT2B13 and UGT2B16. Whereas the UGT2B16-13 chimera retained activity and the substrate selectivity characteristic of UGT2B16, UGT2B13-16 lacked activity. Similarly, a UGT2B13-16 chimera that incorporated only the 97 carboxyl terminal residues of UGT2B16 lacked activity, although a UGT2B13-$16_{(300–358)}$-13 hybrid exhibited activity, albeit relatively low. The results of the present study are broadly consistent with these previous observations. In particular, residues throughout the UGT2B7 sequence, or at least to position 468, appear to be necessary for 'normal' catalytic activity of this enzyme. The reason for this is currently unknown.

In summary, residues 60–194 of UGT2B15 are apparently responsible for substrate binding and for conferring the unique substrate selectivity of this enzyme. The glucuronidation of several UGT2B7 substrates, such as 4MU, exhibit sigmoidal kinetics consistent with the simultaneous binding of two substrate molecules within the active site. In the present study, sigmoidal 4MU glucuronidation kinetics was associated with UGT2B7-15 chimeric proteins that incorporated amino acids 158–197 of UGT2B7. Whether this region of UGT2B7 represents a dimerization domain is currently under investigation.

Acknowledgements

Technical assistance from Kushari Bowalgaha, Edward Chie, Xiao-Hui Guo and the late Wendy McKinnon is gratefully acknowledged. This work was supported by a grant from the National health and Medical Research Council of Australia.

REFERENCES

[1] Tukey RH, Strassburg CP. Human UDP-glucuronosyltransferases: metabolism, expression, and disease. Annu Rev Pharmacol Toxicol 2000;40:581–616.
[2] Miners JO, Mackenzie PI. Drug glucuronidation in humans. Pharmacol Ther 1991;51:347–69.
[3] Radominska-Pandya A, Czernik PJ, Little JM, Battaglia E, Mackenzie PI. Structural and functional studies of UDP-glucuronosyltransferases. Drug Metab Rev 1999;31:817–99.
[4] Mackenzie PI, Bock KW, Burchell B, Guillemette C, Ikushiro SI, Iyanagi T, et al. Nomenclature update for the

mammalian UDP glycoslytransferase (UGT) gene superfamily. Pharmacogenet Genomics 2005;15:677–85.
[5] Miners JO, Smith PA, Sorich MJ, McKinnon RA, Mackenzie PI. Predicting human drug glucuronidation parameters: application of in vitro and in silico modeling approaches. Annu Rev Pharmacol Toxicol 2004;44:1–25.
[6] Ouzzine M, Barre L, Netter P, Magdalou J, Fournel-Gigleux S. The human UDP-glucuronosyltransferases: structural aspects and drug glucuronidation. Drug Metab Rev 2003;35:287–303.
[7] Owens IS, Ritter JK. The novel bilirubin phenol UDP-glucuronosyltransferase UGT1 gene locus—implications for multiple nonhemolytic familial hyperbilirubinemia phenotypes. Pharmacogenetics 1992;2:93–108.
[8] Mackenzie PI. Expression of chimeric cDNAs in cell-culture defines a region of UDP glucuronosyltransferase involved in substrate selection. J Biol Chem 1990;265:3432–5.
[9] Li Q, Lou XJ, Peyronneau MA, Straub PO, Tukey RH. Expression and functional domains of rabbit liver UDP-glucuronosyltransferase 2B16 and 2B13. J Biol Chem 1997;272:3272–9.
[10] Ritter JK, Chen F, Sheen YY, Lubet RA, Owens IS. Two human liver cDNAs encode UDP-glucuronosyltransferases with 2 log differences in activity toward parallel substrates including hyodeoxycholic acid and certain estrogen derivatives. Biochemistry 1992;31:3409–14.
[11] Coffman BL, Kearney WR, Green MD, Lowery RG, Tephly TR. Analysis of opioid binding to UDP-glucuronosyltransferase 2B7 fusion proteins using nuclear magnetic resonance spectroscopy. Mol Pharmacol 2001;59:1464–9.
[12] Coffman BL, Kearney WR, Goldsmith S, Knosp BM, Tephly TR. Opioids bind to the amino acids 84 to 118 of UDP-glucuronosyltransferase UGT2B7. Mol Pharmacol 2003;63:283–8.
[13] Dubois SG, Beaulieu M, Levesque E, Hum DW, Belanger A. Alteration of human UDP-glucuronosyltransferase UGT2B17 regio-specificity by a single amino acid substitution. J Mol Biol 1999;289:29–39.
[14] Jin C, Miners JO, Lillywhite KJ, Mackenzie PI. Complementary deoxyribonucleic acid cloning and expression of a human liver uridine diphosphate-glucuronosyltransferase glucuronidating carboxylic acid-containing drugs. J Pharmacol Exp Ther 1993;264:475–9.
[15] Coffman BL, King CD, Rios GR, Tephly TR. The glucuronidation of opioids, other xenobiotics, and androgens by human UGT2B7Y(268) and UGT2B7H(268). Drug Metab Dispos 1998;26:73–7.
[16] Kiang TKL, Ensom MHH, Chang TKH. UDP-glucuronosyltransferases and clinical drug–drug interactions. Pharmacol Ther 2005;106:97–132.
[17] Green MD, Oturu EM, Tephly TR. Stable expression of a human liver UDP-glucuronosyltransferase (UGT2B15) with activity toward steroid and xenobiotic substrates. Drug Metab Dispos 1994;22:799–805.
[18] Court MH, Duan SX, Guillemette C, Journault K, Krishnaswamy S, Von Moltke LL, et al. Stereoselective conjugation of oxazepam by human UDP-glucuronosyltransferases (UGTs): S-oxazepam is glucuronidated by UGT2B15, while R-oxazepam is glucuronidated by UGT2B7 and UGT1A9. Drug Metab Dispos 2002;30:1257–65.
[19] Chung JY, Cho JY, Yu KS, Kim JR, Jung HR, Lim KS, et al. Effect of the UGT2B15 genotype on the pharmacokinetics, pharmacodynamics, and drug interactions of intravenous lorazepam in healthy volunteers. Clin Pharmacol Ther 2005;77:486–94.
[20] Turgeon D, Carrier JS, Levesque E, Hum DW, Belanger A. Relative enzymatic activity, protein stability, and tissue distribution of human steroid-metabolizing UGT2B subfamily members. Endocrinology 2001;142:778–87.
[21] Uchaipichat V, Mackenzie PI, Guo XH, Gardner-Stephen D, Galetin A, Houston JB, et al. Human UDP-glucuronosyltransferases: isoform selectivity and kinetics of 4-methylumbelliferone and 1-naphthol glucuronidation, effects of organic solvents, and inhibition by diclofenac and probenecid. Drug Metab Dispos 2004;32:413–23.
[22] Bauman JN, Goosen TC, Tugnait M, Peterkin V, Hurst SI, Menning LC, et al. UDP-glucuronosyltransferase 2B7 is the major enzyme responsible for gemcabene glucuronidation in human liver microsomes. Drug Metab Dispos 2005;33:1349–54.
[23] Monaghan G, Clarke DJ, Povey S, See CG, Boxer M, Burchell B. Isolation of a Human Yac contig encompassing a cluster of UGT2 genes and its regional localization to chromosome 4q13. Genomics 1994;23:496–9.
[24] Sorich MJ, Smith PA, McKinnon RA, Miners JO. Pharmacophore and quantitative structure activity relationship modelling of UDP-glucuronosyltransferase 1A1 (UGT1A1) substrates. Pharmacogenetics 2002;12:635–45.
[25] Hobbs S, Jitrapakdee S, Wallace JC. Development of a bicistronic vector driven by the human polypeptide chain elongation factor 1α promoter for creation of stable mammalian cell lines that express very high levels of recombinant proteins. Biochem Biophys Res Commun 1998;252:368–72.
[26] Mackenzie PI, Hjelmeland LM, Owens IS. Purification and immunochemical characterization of a low-pI form of UDP glucuronosyltransferase from mouse liver. Arch Biochem Biophys 1984;231:487–97.
[27] Houston JB, Kenworthy KE. In vitro–in vivo scaling of CYP kinetic data not consistent with the classical Michaelis–Menten model. Drug Metab Dispos 2000;28:246–54.
[28] Barbier O, Turgeon D, Girard C, Green MD, Tephly TR, Hum DW, et al. 3′-azido-3′-deoxythimidine (AZT) is glucuronidated by human UDP-glucuronosyltransferase 2B7 (UGT2B7). Drug Metab Dispos 2000;28:497–502.
[29] Jin C-J, Mackenzie PI, Miners JO. The regio- and stereo-selectivity of C19 and C21 hydroxysteroid glucuronidation by UGT2B7 and UGT2B11. Arch Biochem Biophys 1997;341:207–11.
[30] Meech R, Mackenzie PI. UDP-glucuronosyltransferase, the role of the amino terminus in dimerization. J Biol Chem 1997;272:26913–7.
[31] Ikushiro S, Emi Y, Iyanagi T. Protein–protein interactions between UDP-glucuronosyltransferase isozymes in rat hepatic microsomes. Biochemistry 1997;36:7154–61.
[32] Ishii Y, Miyoshi A, Watanabe R, Tsuruda K, Tsuda M, Yamaguchi-Nagamatsu Y, et al. Simultaneous expression of guinea pig UDP-glucuronosyltransferase 2B21 and 2B22 in COS-7 cells enhances UDP-glucuronosyltransferase 2B21-catalyzed morphine-6-glucuronide formation. Mol Pharmacol 2001;60:1040–8.
[33] Kurkela M, Garcia-Horsman JA, Luukkanen L, Morsky S, Taskinen J, Baumann M, et al. Expression and characterization of recombinant human UDP-glucuronosyltransferases (UGTs). J Biol Chem 2003;278:3536–44.
[34] Ghosh SS, Sappal BS, Kalpana GV, Lee SW, Chowdhury JR, Chowdhury NR. Homodimerization of human bilirubin-uridine-diphosphoglucuronate glucuronosyltransferase-1 (UGT1A1) and its functional implications. J Biol Chem 2001;276:42108–15.
[35] McLure JA, Miners JO, Birkett DJ. Non-specific binding of drugs to human liver microsomes. Br J Clin Pharmacol 2000;49:453–61.